

LOWERING COSTS BY SIMULATING DESIGN OF COMPLEX WELDS

DESIGN OF AN INDENT-FREE INDIRECT RESISTANCE PROJECTION HEM WELD ON AHSS USING SIMULATION SOFTWARE

Kevin R. Chan¹, Pete Edwards²

1. Huys Welding Strategies Ltd., Weston, Ontario Canada
2. Honda Engineering North America Inc, Marysville, Ohio USA

ABSTRACT

Resistance weld surface appearance can be critical in applications where the outer surface is exposed. The joining of multiple sheet stack-ups can exhibit electrode indentation deformation to the worksheets at the electrode-work surface interface requiring rework. The deformation is due to heat input and electrode force. With the emergence of advanced high strength steels (AHSS), weld forces and heat input have had to be increased, leading to an increased tendency for indentation. Limiting the extent of electrode indentation is traditionally managed by controlling the heat balance and electrode size. Shifting the heat balance of the weld can lead to loss of weld quality and size. Indirect resistance projection welding is able to manage the heat generation on a sensitive surface while focusing the heat to the faying surface. Investigation of a specific hem weld geometry using AHSS was carried out using three proposed projection geometries. SORPAS® resistance welding simulation software was used to model the physical deformation as well as heat generation and weld nugget growth. Projection geometry design was compared and optimized by simulation to maximize the size of the weld nugget while minimizing the deformation experienced on the outer surface. Simulations predicted the *Type C* projection design to exhibit no deformation on the outer surface when weld parameters were optimized. This projection design was able to form a nugget large enough to meet all applicable weld requirements. Simulation results were used to eliminate other possible projection geometries based on insufficient weld quality or indentation on the outer surface.

An independent lab tested the preferred joint design versus the simulation results for joint quality and surface deformation. Welding results showed the simulations were within a test range with respect to deformation and nugget size. The correlation of the simulation with actual condition allows both cost and time savings in the automotive industry. This suggests that Sorpas® can advance joint design capability for OEM's that use a short design-to-mass-production timeframe.

INTRODUCTION

The use of resistance welding for the joining of sheet metals in the automotive industry is very widespread due to the ease of maintenance, low cost, and ease of automation of the process. The process involves clamping the work sheets together between the electrodes, applying a weld force, and the weld current to generate enough heat to cause melting and coalescence of the sheets forming a sound fusion joint. Traditional resistance spot welding is shown in Figure 1, and uses electrodes on the top and bottom of the sheets to be welded. This is beneficial because the heating is balanced between the sheets at the interface where it is most needed. In this type of direct resistance welding, the current passes from one electrode through the work

sheets, and to ground via the second electrode. The necessary weld force is also applied by the electrodes, generating the weld pressure needed to breakdown the interfaces and contain the molten weld nugget as heating is applied. With the electrodes carrying both weld current and force, the system is simplified; however this combination also leads to electrode indentation and deformation of the work sheets. For most weld applications, this surface marking is acceptable, or removed with secondary operations such as grinding when the surface condition is critical. With the emergence of advanced high strength steels (AHSS), weld forces and heat input have had to be increased to successfully weld the materials, leading to an increased tendency for indentation.

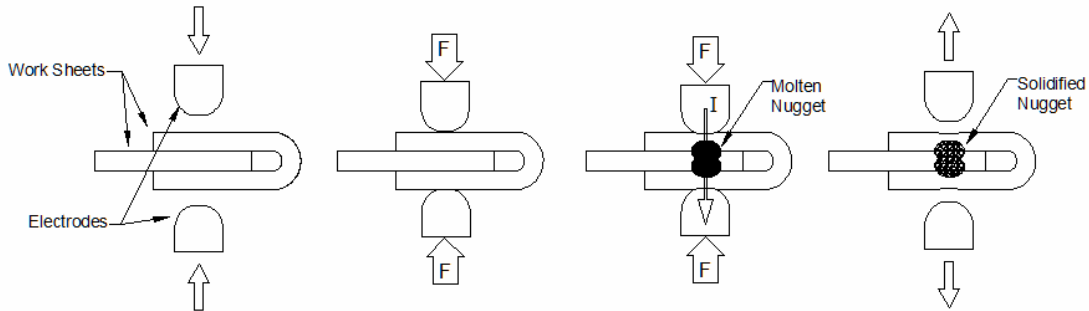


Figure 1: Schematic diagram of RSW process

Resistance weld surface appearance can be critical in applications where the outer surface is exposed as a finished product. Limiting the extent of electrode indentation is traditionally managed by controlling the heat balance and electrode size. By moving the weld nugget away from the critical surface, sheet softening and resultant indentation can be reduced. This can be done by sizing the electrodes so that the larger contact face is on the sheet surface that is critical. The larger electrode also conducts heat away at a higher rate due to its greater thermal mass and contact area. Shifting the heat balance of the weld leads to loss of weld quality and size and asymmetric electrodes can be installed improperly leading to excessive indentation on the critical surface.

Indirect resistance welding is the resistance welding process where the weld force and weld current are carried by different electrodes. While the weld force is applied in a similar manner as traditional direct RSW, the weld current is directed along a different path so that a critical interface can be excluded from the current path and heating reduced. This can be achieved by grounding the current path through another tool that has good contact with the worksheets. Fixturing and location jigs can be used to redirect the current path away from the critical interface. Such a setup is shown in Figure 2, where the top and bottom electrodes apply the weld force, and the top electrode conducts the weld current through the top sheet and faying interface, and then is grounded through the tertiary electrode.

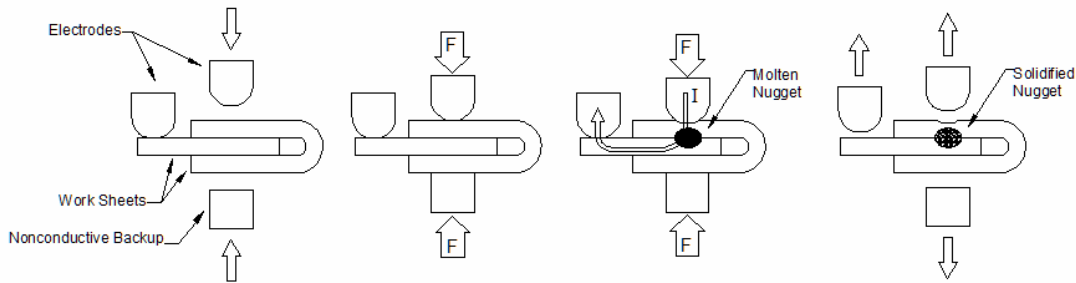


Figure 2: Schematic diagram of Indirect RSW process

Indirect welding can also cause problems with current shunting and imbalanced heating when welding complex stack-ups. For welding automotive door hem joints requiring an indent free outer surface, simple indirect welding is not able to form a sound weld while eliminating deformation on the outer surface. The current shunting through the radius of the hem joint is too great. To address this issue, indirect projection welding is able to manage the heat generation on a sensitive surface while focusing the heat to the faying surface by presenting a raised projection. Design and optimization of this projection geometry was done with the assistance of Sorpas® resistance welding simulation software. Projection designs were compared through simulation of indirect projection hem welds while tracking nugget size and critical surface heating and deformation. Requirements for the size of the nugget were adapted from AWS standards [Ref. 1] and are shown in Table 1.

Table 1: Nugget size requirements for Projection Hem welding

Sheet Thickness	Minimum	Maximum
(mm)	(mm)	(mm)
0.7	2.5	4

EXPERIMENTAL PROCEDURES

Creating the simulation

All simulations were carried out on FEA software *SORPAS®* from *Swantec Software and Engineering ApS* [Ref. 2]. The process for creating a simulation is shown in Figure 3. Welding electrodes and work sheet configurations are entered into the simulation using a 2D co-ordinate mapping system to create objects. A materials database is then used to assign the object material properties as shown in Figure 4. Once the objects have been designed and assigned properties, the machine tools are specified to apply the weld force and current. A mesh of nodes is applied to the 2D image. Given the configuration used for the simulation it is required to have a minimum of 1000 nodes. The weld force and current can be characterized to match existing welding machines and controllers. At this stage, all welding parameters can be specified in the simulation. Finally, the simulation parameters can be adjusted to change simulation speed and accuracy. Automatic optimizations can also be setup to iterate simulations to find a specific weld nugget size or current range for weld lobe studies. Simulation parameters used in this study are shown in Table 2.

Indirect resistance spot welding was achieved in the simulation by moving the electrical ground tool to the inner hem sheet. The insertion of a non-conductive layer on the lower anvil tool was used to prevent grounding. Projections were designed with simple geometries adapted from the ASM standards for resistance welding projections [Ref. 3].

SORPAS (R) Version 6.6 Enterprise Edition
Copyright (C) 1995-2005 by SWANTEC Software and Engineering ApS. All rights reserved.

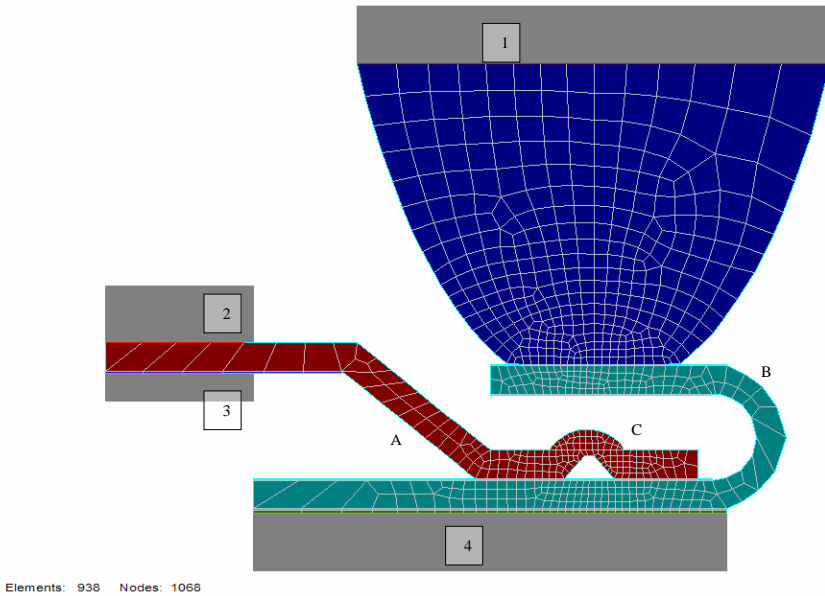


Figure 3: Simulation object schematic. Objects 1-4 are machine tools. A, B, and C are work pieces hem-inner, hem-outer, and hem-projection respectively.

SORPAS - [h-steel 316-lik.kobec.dat]

File Input Mesh Simulation Batch Run Optimization Results View Database Help

Material Database: Load Material from Database File Save Cancel OK

Remove Add New Duplicate Remove Add New Duplicate ID: 236 227

Category: High Strength Steels Material: HSLA 350

Name: High Strength Steels Name: HSLA 350

HAZ T: 780.000 [°C] Solidus: 1500.000 [°C] Liquidus: 1510.000 [°C] Latent Heat of Fusion: 277.000 [kJ/kg]

Property	20.000	100.000	200.000
Thermal Conductivity	51.900	51.700	50.000
T [°C], TC [W/mK]			
Heat Capacity	472.000	506.000	522.000
T [°C], HC [J/kg K]			
Mass Density	8020.000		
T [°C], MD [kg/m³]			
Resistivity	0.174	0.194	0.256
T [°C], R [µ-Ohm-m]			
Surface Contaminants Resistivity	40.000	27.000	12.000
T [°C], R _c [µ-Ohm-m]			
Thermal Expansion Coefficient	11.900	12.700	13.900
T [°C], TEC [10 ⁻⁶ /°C]			
Young's Modulus of Elasticity	200.000		
T [°C], E [GPa] [GPa = kN/mm²]			
Poisson's Ratio	0.300		
T [°C], PR			
Flow Stress Curve	0.000 0.150 0.100	0.000 0.150 0.080	0.000 0.340 0.070
T [°C], C [MPa], B, n, m [FS = Cσ + B]ⁿ m σ⁻ᵐ			

Figure 4: Sample Materials property screen for Sorpas® displaying static and temperature dependent material properties for HSLA 350 Steel.

The critical aspects for creating a simulation for this project were to develop a model that would take into account the primary and secondary variables of the system. The primary welding variables for this simulation are the Current, Weld Time, Squeeze Force, and projection height. The secondary variables are the distance from the weld to the ground, electrode shape, and the anvil material. Since the purpose of this testing was to develop an optimized projection for a hem weld, the focus was on the projection height. Adaptations from work by Sun on modeling projection heights were used for initial design [Ref 4,5]. Three heights were considered and simulated for the projection welds. These were put through simulated parameter development to obtain the optimized parameters.

Table 2: Simulation Parameters

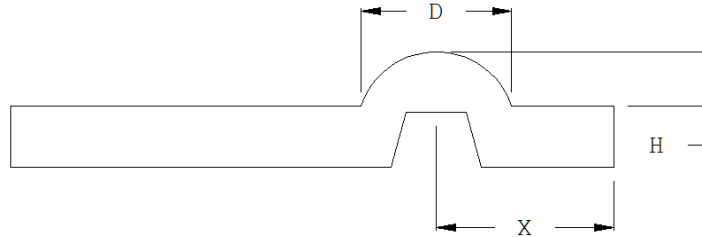
Simulation Parameters				
	Squeeze	Weld	Hold	
Time Step Increment	0.1	0.05	0.1	(ms)
Save Data Per	10	5	10	steps
Convergence Control				
	Convergence Accuracy			
Electrical Model	1.00E-05			
Thermal Model	1.00E-05			
Mechanical Model	1.00E-05			
Dynamic Contact Between Materials				
	Sliding			
Heat Loss to Surroundings				
Air Temperature	20			°C
Heat Transfer Rate	300			(W/m ² K)

Design Parameters

Worksheet materials were 0.7mm JAC270 steel with a tensile strength of 270MPa commonly used for door panels and 0.7mm DP600 steel supplied by *Dofasco*. Hem joint outer sheets were made of the JAC270 while the inner sheets were of the DP600 material. The objective of the design was to create a geometry and weld schedule that would achieve an acceptable weld nugget between the hem outer-upper section and the hem inner section without applying excessive heat and pressure to the hem outer-lower sheet or Hem edge as to produce sheet deformation. RWMA Class 2 CCZ electrode material was used for top and bottom electrodes. Parabolic (Paracap™ [Ref 6]) electrode geometry was used on the top electrode (moving) with a 6mm weld face. A 140mm diameter flat electrode was used as the anvil electrode with a non-conductive layer between the anvil and the steel. Grounding of the circuit was through a secondary electrode in contact with the inner hem sheet away from the joint area.

Simulations were conducted with three levels of weld force: 1.0 kN for Low, 1.75 kN for Medium, and 2.5 kN for High force. Projection designs are shown as entered in the simulation in Figure 5. Weld current windows were then found for each of these force settings and then the entire process was repeated for each of the three projection heights used. Acceptable nuggets were qualified according to AWS standards for projection welded joints [Ref 1] and shown in Table 1. Results for the simulated weld lobe based on current and squeeze force were tabulated and

evaluated on weldability. Lobe boundaries were defined as the 2.5mm nugget for the lower limit and the point at which the nugget grows into the hem-inner flange, or the point where the hem-outer lower flange experiences a temperature greater than 723 °C. This is the ferrite to austenite eutectoid temperature of the steel. Overheating of the inner flange is shown in Figure 6 where melting has occurred away from the faying interface. For the purposes of testing the weld time was kept constant at 6 cycles of AC current.



	Type A	Type B	Type C	
D	2.5	2.5	2.5	(mm)
H	0.7	0.9	1.1	(mm)
X	5.0	5.0	5.0	(mm)

Figure 5: Hem-inner Projection Schematic

Simulations yielding passing weld nuggets were then analyzed for outer surface indentation. Peak temperatures of the hem-outer lower sheet were monitored at the electrode-sheet interface along with any node movement which would indicate indentation of the sheet. Maximum allowable temperature for the outer surface of the hem was set at 723°C also to avoid the chance of material softening and deformation [Ref 7].

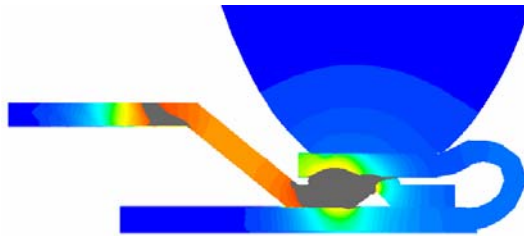


Figure 6: Overheat condition of welds outside of the acceptable current limit. Note the heating of the hem-inner and the lower hem-outer flange.

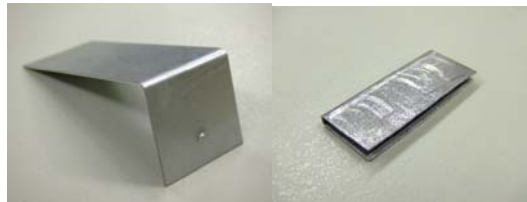
Laboratory Welding

All lab testing was conducted on a 250kVA single phase AC pedestal welder modified for indirect resistance spot welding. The indirect welding setup is shown in Figure 7. Welding parameters were entered as specified by simulation results and welds were made on hem coupons fabricated to match the simulation geometries in the hem section. Current path grounding was achieved by modification of the lower electrode and inner hem sheet to allow the lower electrode to apply the weld force to the joint, but shunt the current through the inner hem sheet only. Hem coupon dimensions used for laboratory testing were identical for each test. Projections were stamped on hem coupons as specified by Fig 5. Hem coupon dimensions are

given in Figure 8. Welds were then cross sectioned and etched then analyzed using optical microscopy. Nugget sizes were measured from the cross sections as well as heating artifacts as noted by changes to the grain structure of the material.



Figure 7: Image showing laboratory setup for indirect hem welding. The hem-inner has been bent to make electrical contact with the lower electrode. The hem-outer is insulated from the lower electrode with a nonconductive material.



Hem-Inner	(mm)	Hem-Outer	(mm)
D	2.5	Flange Length	30.0
H	0.7	Curve Radius	2.0
X	5.0		

Figure 8: Hem Dimensions for laboratory testing

RESULTS AND DISCUSSION

Simulation Results

Weld Lobes

Three types of weld projections were proposed for the design of a new indirect welding application. Simulation of welds produced by the three types of projections at three levels of weld force, over a range of weld currents was conducted yielding weld current and force lobes at a constant weld time. Weldability lobes for the three different projection heights are given in Figures 9, 10, and 11. Both Nugget Size vs. Weld current and Weld Force vs. Weld Current

plots are given in the figures. For all three of the projection designs, there seemed to be a very clear threshold of weld current that would cause melting in the inner sheet. This is due to the fact that the inner worksheet is independent of the projection design and is identical for all three projection types. The nugget size vs. current plots all show that lower weld force yields larger nuggets at lower current as expected with resistance welding. Usable current ranges for all three types of projections fell between 4 and 6kA of current. Below this range, the nugget is undersized, and above this range excessive heating of the hem-inner occurs as it is acting as a shunt to the indirect electrode. The plots also show that as the projection height is increased, the final nugget size before overheating was also increased. The Type C projection was able to form the largest nuggets before overheating.

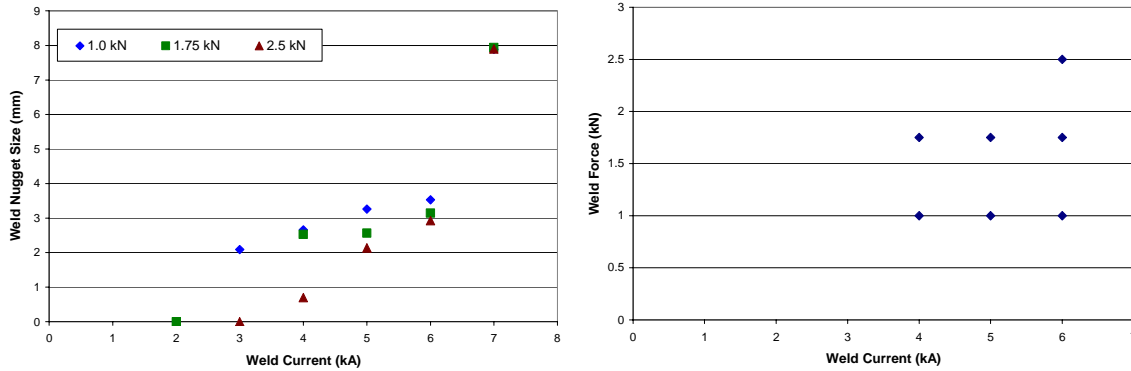


Figure 9: Projection Type A: Left- Weld Nugget Size Curves, Right- Weld Lobe

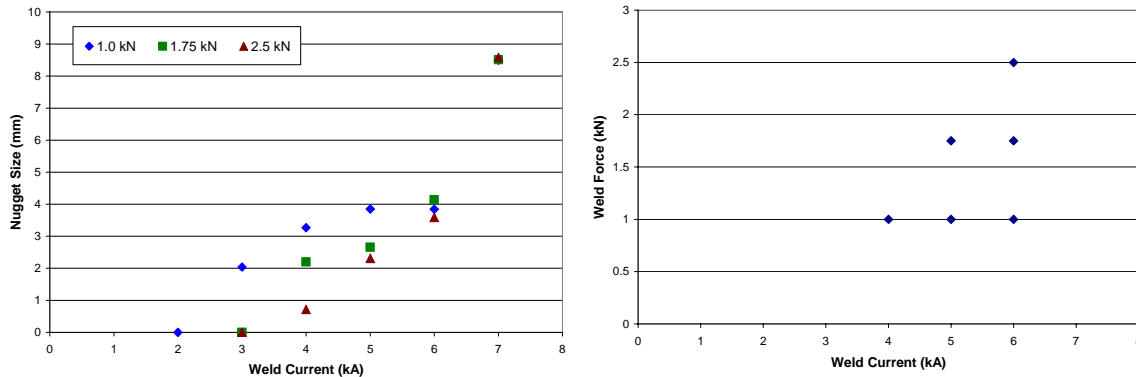


Figure 10: Projection Type B: Left- Weld Nugget Size Curves, Right- Weld Lobe

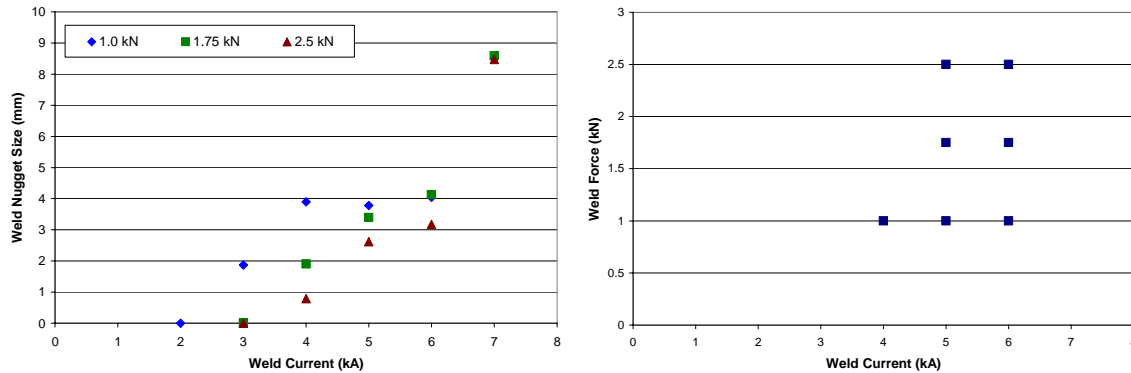


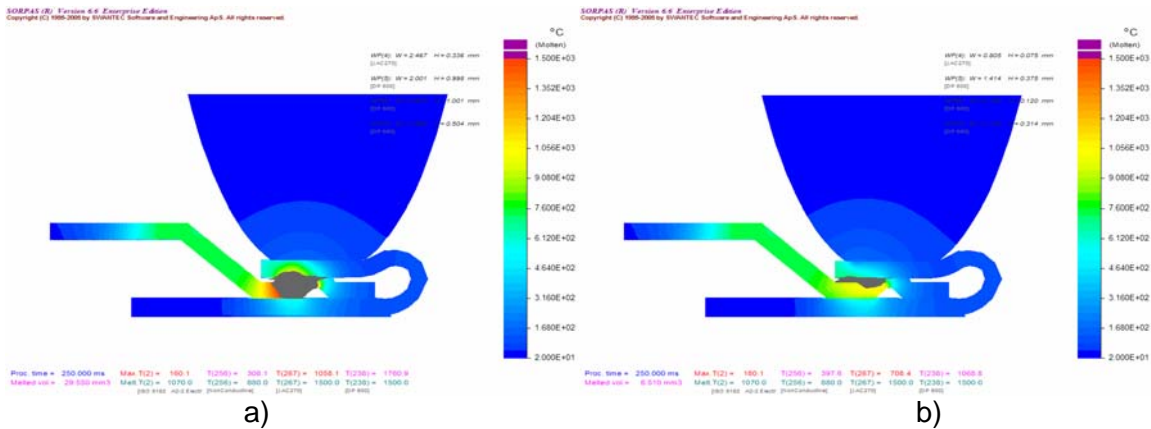
Figure 11: Projection Type C: Left- Weld Nugget Size Curves, Right- Weld Lobe

Weld Profile

To further compare the types of projections, the shape and penetration of the best case weld nuggets as predicted by the simulation software were studied in an effort to determine the best projection design for the weld. Predictions for nugget shape were taken from the largest nugget before overheating at each weld force setting for each of the projection types. Figures 12, 13, and 14 show the welds for each of the three projection types A, B, and C respectively. It is clear that the nugget size value reported by the simulation alone is not a good indicator of weld quality. Weld penetration into the hem-upper section along with the corresponding weld nugget diameter is given in Table 3 and shows that the Type C projection is the most consistent at medium to low force.

Table 3: Predicted weld penetration into hem-upper flange and corresponding nugget diameter.

Projection Type		Weld Force		
		2.5kN	1.75kN	1.0kN
Type A	Penetration (mm)	0.175	0.075	0.336
	Diameter (mm)	2.925	3.142	3.53
Type B	Penetration (mm)	0.045	0.227	0.245
	Diameter (mm)	3.589	4.142	3.844
Type C	Penetration (mm)	0.09	0.223	0.232
	Diameter (mm)	3.177	4.13	4.039



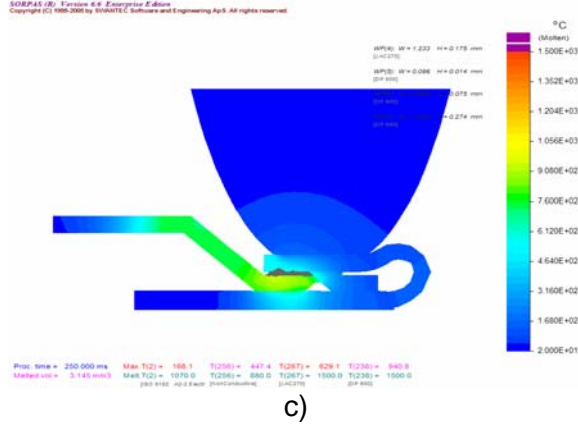


Figure 12: Type A Projection welds; a) Low force weld. Nugget diameter = 3.53mm; b) Medium force weld. Nugget diameter = 3.142mm; c) High force weld. Nugget diameter = 2.925mm

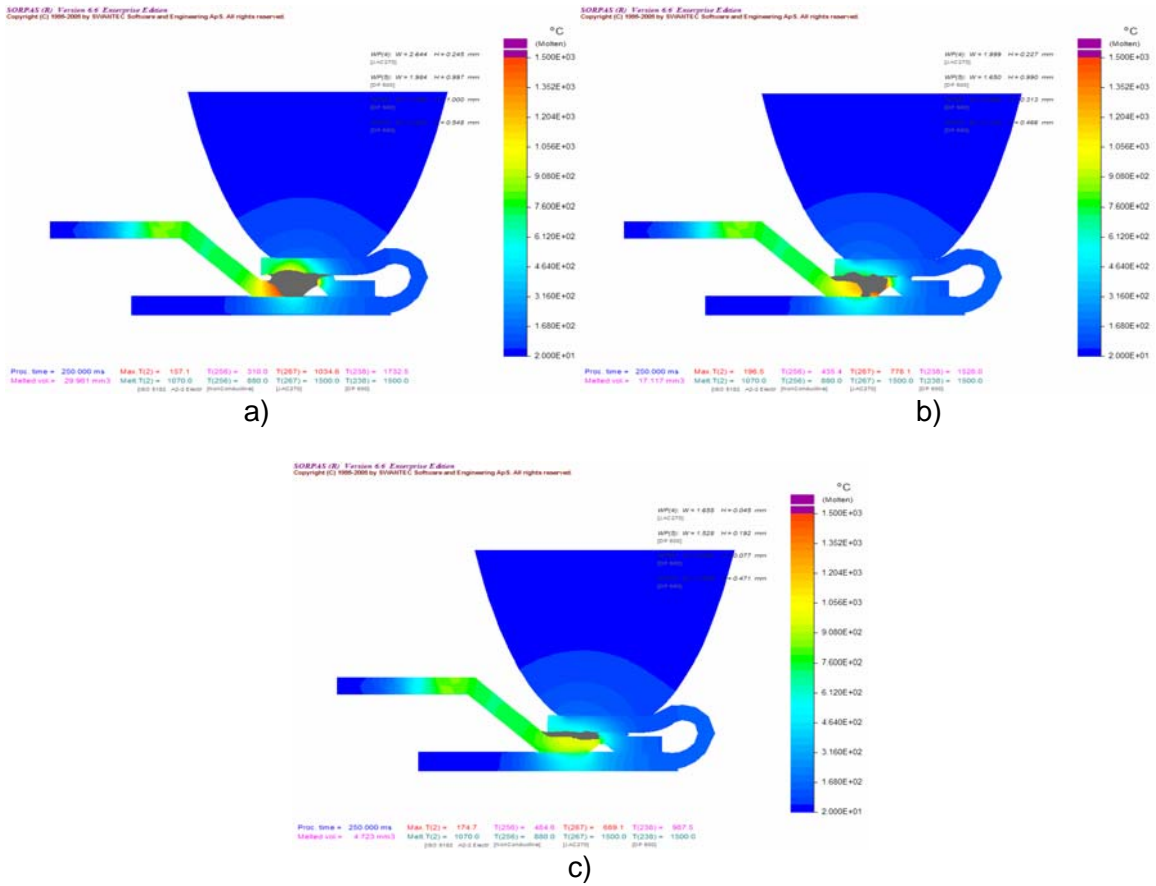


Figure 13: Type B Projection welds; a) Low force weld. Nugget diameter = 3.844mm; b) Medium force weld. Nugget diameter = 4.142mm; c) High force weld. Nugget diameter = 3.589mm

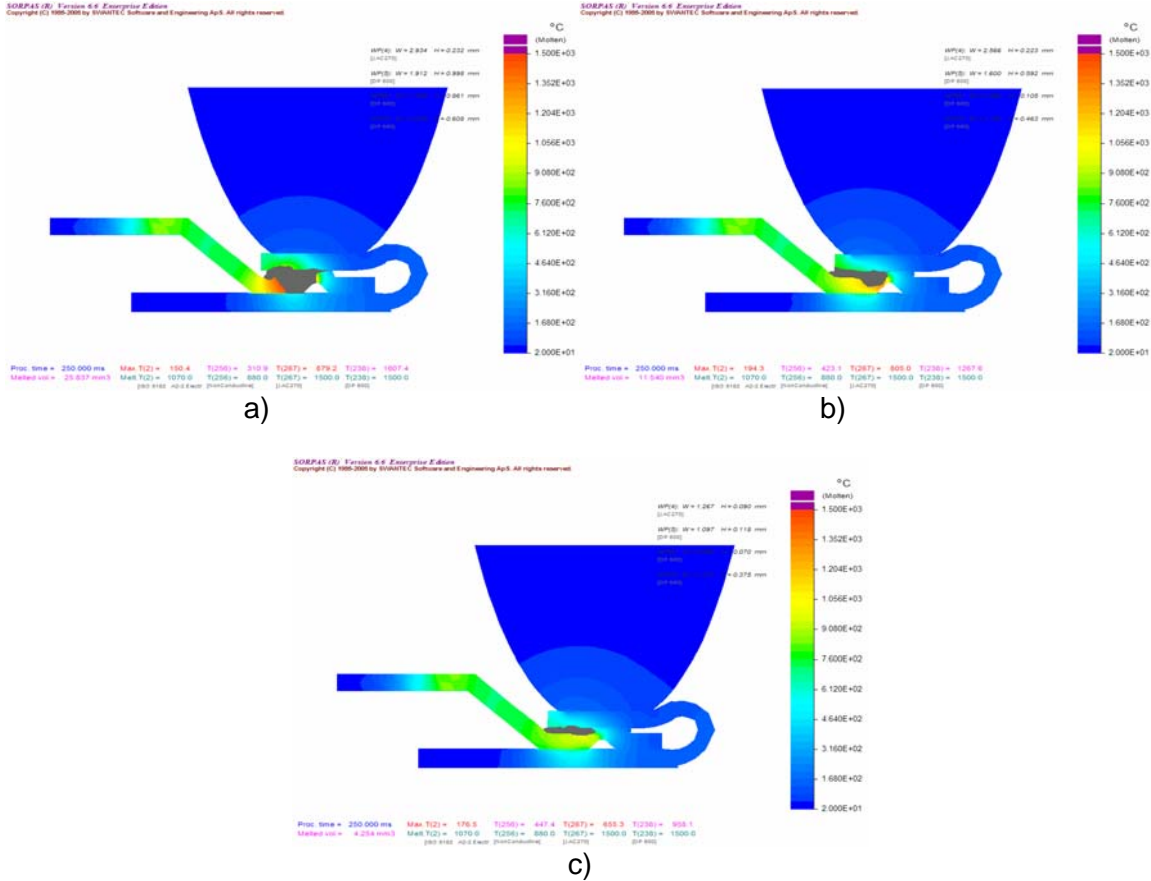


Figure 14: Type C Projection welds; a) Low force weld. Nugget diameter = 4.039mm; b) Medium force weld. Nugget diameter = 4.130mm; c) High force weld. Nugget diameter = 3.177mm

Selected Projection Design

From the simulation results, the Type C projection was chosen as the best projection design of the three presented as it possessed the largest weld lobe with acceptable welds along with good penetration and weld diameter without excessive heating of the lower flange. From the weldability lobes generated by simulation, the optimal welding schedule for the chosen Type C projection has been determined to be 6kA for 6 cycles at a weld force of 1.75kN. This schedule was chosen based on the upper end of the weldability lobe providing enough heat ensure a weld nugget has formed while attempting to minimize the amount of expulsion generated.

Lab Testing Results

From the simulation results, the chosen projection design was tested using the suggested weld schedule. Figure 15 shows the weld after cross sectioning and etching, the fusion zone can be seen between the hem-inner and the hem-outer upper sheets. The lower section of the hem has not experienced enough heating to affect the microstructure of the steel. Some expulsion was experienced at the beginning of the weld as is normally seen with projection welding. Inspection of the bottom surface of the hem-outer sheet revealed no notable marking or deformation. Although the position of the nugget is slightly shifted from that of the predicted position of the nugget, the approximate size is very similar. The shift was due to a slight

misalignment of the projection and the electrodes. Note however that the weld nugget has formed on half of the projection, and the other half remains unfused, as predicted by the simulation. Also the amount of collapse of the projection is very similar to the predicted degree. As this study was not aimed at detailed verification of the simulation predictions, the initial results are promising in that simulations were able to provide welding schedules and behavior very close to that of the actual weld with very little testing being carried out.

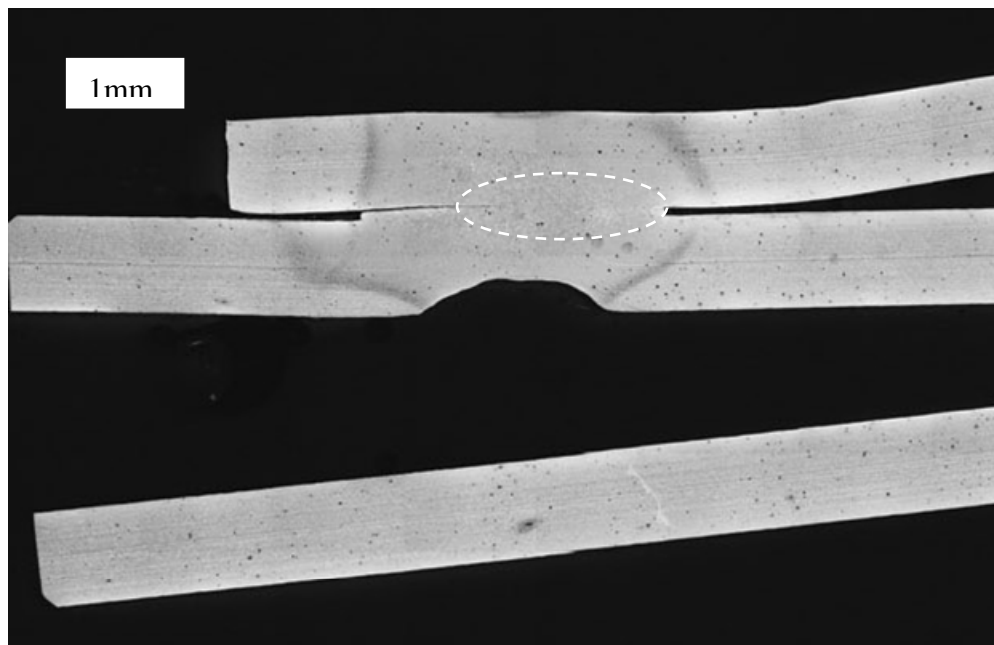
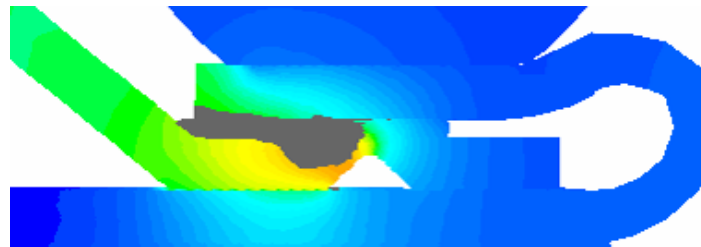


Figure 15: Laboratory weld comparison. Top- Simulation result for Type C projection. Bottom- Cross sectioned indirect hem weld using Type C projection and weld parameters from simulation. The lower layer does not show deformation or a Heat Affected Zone. The separation is due to spring back from the Hemming and welding process.

Rapid Design with Weld Simulations

By conducting weldability lobes and nugget size and shape studies for the projection designs by using simulation, actual lab testing was greatly reduced while demonstrating that the new design for an indirect indent free hem weld was possible. The cost to benefit ratio for simulating the design is sufficient for continuing this process, but the benefit of starting with a design and parameters that can be directly applied to welding equipment is even more significant. For the purposes of this testing the hours spent simulating versus the hours used for testing samples was not tracked. However, once a proven simulation technique and set up has been created, modifying it for different circumstances and stacks is significantly quicker than testing.

CONCLUSIONS

A new design for an indirect-resistance spot weld of a three-sheet hem weld was explored using Sorpas® resistance welding software and laboratory welding. This work shows the study of the modeling and simulation of a specific type of projection welding used in the automotive industry. Projection height and weld force were tested using simulations and presented. The Type C projection (1.1mm high) coupled with medium weld force (1.75kN) was found to yield the best quality of welds and reliability. Laboratory testing was then conducted only on the selected projection configuration and weld schedule to confirm simulation findings. Correlation between the model simulation and lab testing was sufficient to validate the design process tool of software modeling and simulation of this particular joint design.

The use of simulation software to develop better welding projections is important to assist automotive design groups to increase quality while maintaining or reducing development costs. Since design to production timing is being reduced for the global manufacturing community every possible technique must be used to develop welding and welding related designs as early as possible. In the case of the Hem flange welds, these are A class welds that will be seen by the customers and must be of the highest quality. This study shows that not only can these welds be predicted, but the quality can be improved early enough in the design timing to allow changes and improvements to be made at little to no cost.

The testing of the sample components did show some differences to the simulation. As was previously mentioned, there was some misalignment in the electrodes on the test set up. This is important to keep in mind while simulating welds. The “real world” equipment will have differences that can not be simulated. That is not to say that simulation is neither accurate nor useful. The method for simulating should be the same as that used in a laboratory setting. 1. Develop the largest weld lobe possible with the given equipment parameters. 2. Recreate the equipment used in mass production as accurately as possible (i.e. electrodes, part gap, etc.). 3. Use consistent procedures for simulation. Using these steps allowed this study to be replicated with existing equipment.

REFERENCES

- (1) ANSI/AWS/SAE/D8.9-97, “Recommended practices for test methods for evaluating the resistance spot welding behaviour of automotive sheet steel materials”, AWS/SAE, 1997
- (2) *Swantec Software and Engineering ApS*, Denmark, www.swantec.com
- (3) Projection Welding, Gould, J E, ASM International, ASM Handbook. Vol. 6: Welding, Brazing, and Soldering (USA), 1993, pp. 230-237, 1993
- (4) Sun, X., Effect of Projection Height on Projection Collapse and Nugget Formation — Finite Element Study, *Welding Journal*, September 2001, p 211-s – 216-s
- (5) Cunningham, A., and Begeman, M. L., 1966. Effect of projection height upon weld quality and strength. *Welding Journal* 45 (1) : 26-s to 30-s.
- (6) Huys Industries Limited, Toronto, Canada, www.huysindustries.com
- (7) *Metals’ Handbook*, 9th ed., Vols. 1 and 2. 1978. Properties and selections: Irons and steels.